

Pressure-dependent ground states and fermiology in β -(BDA-TTP)₂MCl₄ (M =Fe, Ga)

E. S. Choi, D. Graf, and J. S. Brooks

National High Magnetic Field Laboratory, Florida State University, Tallahassee, Florida 32310, USA

J. Yamada and H. Akutsu

Department of Material Science, Graduate School of Science, Himeji Institute of Technology, Hyogo 678-1297, Japan

K. Kikuchi

Department of Chemistry, Graduate School of Science, Tokyo Metropolitan University, Tokyo 192-0397, Japan

M. Tokumoto

*Nanotechnology Research Institute, AIST, Tsukuba 305-8568, Japan**and JST-CREST, Kawaguchi 332-0012, Japan*

(Received 8 January 2004; revised manuscript received 26 March 2004; published 26 July 2004)

We have investigated pressure- and magnetic-field-dependent electrical transport properties in the charge transfer salts β -(BDA-TTP)₂MCl₄ (M =Fe, Ga), both of which show a metal-insulator (MI) transition around 120 K at ambient pressure. The zero field temperature-pressure phase diagrams of the two compounds are quite similar; the MI transition temperature decreases with pressure, and superconductivity is observed in both the magnetic and non-magnetic compounds above \sim 4.5 kbar. Likewise, Shubnikov-de Haas effect measurements show nearly identical Fermi surfaces. These similarities suggest that the magnetic interaction J between the conduction electrons and the magnetic moments in β -(BDA-TTP)₂FeCl₄ is small. Nevertheless, magnetoresistance measurements show remarkable differences and reveal that magnetic interactions with the conduction electrons are still effective in M =Fe compounds.

DOI: 10.1103/PhysRevB.70.024517

PACS number(s): 74.70.Kn, 71.18.+y, 71.20.Rv, 74.25.Dw

I. INTRODUCTION

In organic conductors, the existence of local magnetic moments, usually embedded as magnetic anions, bring in physical phenomena in transport and magnetic properties. For instance, λ -(BETS)₂FeCl₄ [where BETS = bi(ethylenedithio)-tetraselenafulvalene] and its nonmagnetic analogue λ -(BETS)₂GaCl₄ have distinctively different ground states; the former is an antiferromagnetic (AF) insulator while the latter is a superconductor.¹⁻⁵ By applying magnetic field, the insulating state of λ -(BETS)₂FeCl₄ is suppressed and a paramagnetic metallic state is recovered.^{2,5} Furthermore, by applying a magnetic field parallel to the conducting planes, field-induced superconductivity (FISC) is stabilized, which is generally thought to be due to the cancellation of the internal π - d exchange field by the external field^{6,7} (see Sec. IV). Another material that also has magnetic anions and shows FISC behavior is κ -(BETS)₂FeBr₄.⁸⁻¹⁰ This material shows AF ordering at the Néel temperature $T_N=2.5$ K, but remains metallic below T_N , and eventually becomes a superconductor at lower temperatures.¹¹⁻¹³

Given the different cases discussed above, the degree of coupling between π conduction electrons and localized magnetic moments can play an important role in determining the ground state of the system.^{5,14} The coupling constant J is usually expressed in the Kondo Hamiltonian as $J\sum S_i \cdot \sigma_i$, where S_i and σ_i are spin operators for local moments and conduction electrons, respectively. The AF metallic phase of κ -(BETS)₂FeBr₄, therefore, can be attributed to a smaller J in this compound than in λ -(BETS)₂FeCl₄, where strong

π - d coupling localizes the π conduction electrons at $T_N=8.5$ K. An AF metal state was also observed in λ -(BETS)₂FeCl₄ under pressure, which shows successive transitions from a paramagnetic metal to an AF metal, and finally a superconductor at hydrostatic pressures above 3.5 kbar.¹⁵ In general, the effect of pressure is to increase the bandwidth W , thereby changing the balance of the competing ground state energies in the Kondo Hamiltonian.

Recently, in addition to the BEDT-TTF- and BETS-based materials [where BEDT-TTF=bi(ethylenedithio)-tetrathiafulvalene] with TCF (tetrachalcogenafulvalene) structures, non-TCF structured donor molecules, such as BDA-TTP-[2,5-bis(1,3-dithian-2-ylidene)-1,3,4,6-tetrathiapentalene] and BDH-TTP-[2,5-bis(1,3-dithiolan-2-ylidene)-1,3,4,6-tetrathiapentalene] based organic charge transfer salts, have been synthesized.^{16,17} Superconductivity is also observed in these materials and the β -(BDA-TTP)₂SbF₆ superconductor is reported to have the largest effective cyclotron mass ($12.4 \pm 1.1 m_e$) yet found in organic conductors.¹⁸ Among the non-TCF-structured organic conductors, κ -(BDH-TTP)₂FeCl₄ (Ref. 19) and β -(BDA-TTP)₂FeCl₄ (Ref. 20) exhibit metallic conducting behavior in the presence of magnetic ions. While κ -(BDH-TTP)₂FeCl₄ is metallic to 1.5 K without magnetic ordering,¹⁹ β -(BDA-TTP)₂FeCl₄ exhibits a metal-insulator (MI) transition at high temperature (\sim 120 K) and shows AF ordering at $T_N=8.5$ K.²⁰⁻²² The FeCl₄ anion in this compound retains its local magnetic moment $S=5/2$, as do λ -(BETS)₂FeCl₄ and κ -(BETS)₂FeBr₄.

In this paper, we investigate electronic properties of β -(BDA-TTP)₂FeCl₄ and its nonmagnetic isostructural ana-

log β -(BDA-TTP) $_2$ GaCl $_4$,²³ both of which show pressure-induced superconductivity. The primary question is how the pressure-dependent ground state of β -(BDA-TTP) $_2$ GaCl $_4$ changes by introducing magnetic ions. Since the only appreciable difference between β -(BDA-TTP) $_2$ GaCl $_4$ and β -(BDA-TTP) $_2$ FeCl $_4$ is the existence of local magnetic moments, these compounds provide a useful example to study the effect of magnetic interactions in low-dimensional charge transfer salts. The main findings in our work are (i) they have a very similar phase diagram including pressure-induced superconductivity above 4.5 kbar, (ii) the Fermi surfaces of both materials are similar and in agreement with tight binding band calculations, and (iii) the magnetoresistance (MR) of M =Fe is significantly different from M =Ga, indicating that the π - d interaction plays an important role in the electronic transport in M =Fe compounds, and likewise the MR is sensitive to changes in the underlying magnetic order.

II. EXPERIMENTAL DETAILS

β -(BDA-TTP) $_2$ MCl $_4$ (M =Fe, Ga) single-crystal samples are grown by conventional electrochemical methods.^{20,23} The electrical resistance was measured along the interplane direction (crystallographic b axis) with low frequency lock-in techniques. Four gold wires were attached to thin elongated platelike samples using graphite paint. Hydrostatic pressure measurements were done using a self-clamped BeCu pressure cell with a pressure medium of Daphne 7373 oil. Pressure was calibrated with a manganin pressure gauge and high-purity lead.²⁴ The pressure loss during cooling was estimated to be approximately 2 kbar between room temperature and liquid helium temperature. Pressure values reported in this paper are values after consideration of the low temperature loss, unless otherwise indicated. The high magnetic field measurement was done at the National High Magnetic Field Laboratory, Tallahassee, Florida.

III. DATA AND RESULTS

A. Phase diagram

Figure 1 shows the temperature dependence of the resistance ratio $[R(T)/R(290\text{ K})]$ of β -(BDA-TTP) $_2$ FeCl $_4$ and MR data in the low field region at P =9.7 kbar. The room temperature pressure values are used only in this figure in this paper, since the data shown here were taken in the wide range of temperature. The temperature dependence of resistance is similar to the previous report for β -(BDA-TTP) $_2$ GaCl $_4$.²³ The insulating state is significantly suppressed by applying a moderate pressure, and superconductivity eventually appears above a critical pressure P_c (6.5 kbar at room temperature: 4.5 kbar around T_c). The superconductivity is also evident from the MR data shown in the lower inset. At certain pressures, the resistance ratio data exhibit more complex behavior as shown in the upper inset of Fig. 1, where the onsets of the MI transition and superconductivity appear sequentially with decreasing temperatures. The Kondo effect can be ruled out as an explanation for the upturn of resistance, since this behavior was also observed in β -(BDA-TTP) $_2$ GaCl $_4$ samples in a similar pres-

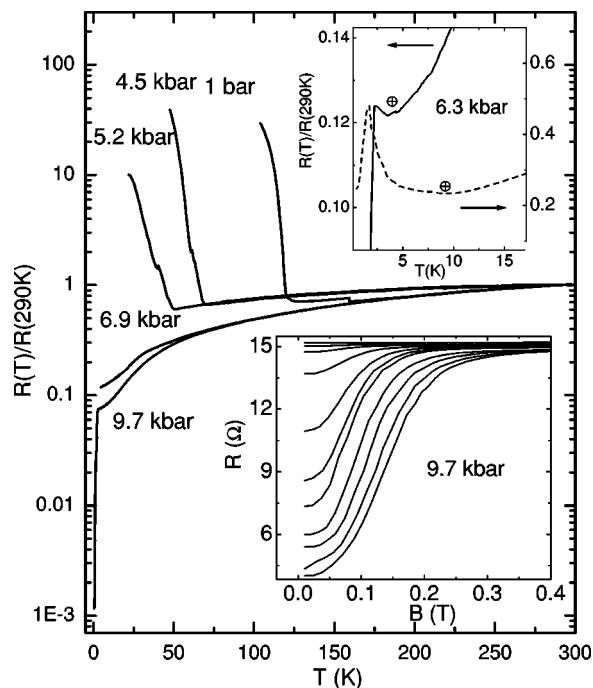


FIG. 1. Temperature dependence of resistance ratio of β -(BDA-TTP) $_2$ FeCl $_4$ at different pressures. Note that the pressure values here are room temperature values. Upper inset: Normalized resistance of two samples measured at 6.3 kbar. \oplus indicates the temperature where the resistance is minimum. Lower inset: Magnetoresistance data for $B\parallel b$ at different temperatures 3, 2.5, 2.2, 1.9, 1.7, 1.5, 1.37, 1.1, 0.9, 0.7, and 0.5 K from top to bottom for the P =9.7 kbar sample. The currents are $1\ \mu\text{A}$ for the cool-down curves and $10\ \mu\text{A}$ for the magnetoresistance data.

sure range.²³ The upturn is more likely just the precursor of the MI transition, which is then shunted when the sample becomes superconducting at lower temperatures. Moreover, the temperature dependence of the upturns of the MI transition shows systematic dependence on increasing pressure. The superconduction (SC) transition of β -(BDA-TTP) $_2$ FeCl $_4$ is not as clear as that of β -(BDA-TTP) $_2$ GaCl $_4$, as it is very broad and maintains a finite resistance even well below the onset temperature of the SC transition. The SC transition is also dependent on the excitation current (the transition is more pronounced for smaller currents) for β -(BDA-TTP) $_2$ FeCl $_4$, while not for β -(BDA-TTP) $_2$ GaCl $_4$.

A temperature-pressure (TP) phase diagram of β -(BDA-TTP) $_2$ MCl $_4$ (M =Fe, Ga) based on the resistance measurement on several samples is shown in Fig. 2. The metal-insulator transition temperature T_{MI} and SC transition temperature T_c were determined from the resistive onsets of the transitions. The overall phase diagram is essentially the same for both compounds, although T_c of β -(BDA-TTP) $_2$ FeCl $_4$ is lower than that of β -(BDA-TTP) $_2$ GaCl $_4$. The pressure effect on T_c is small above P_c for both samples in the range of pressure measured.

It is interesting to note that while the ground states of λ -(BETS) $_2$ MCl $_4$ (M =Fe, Ga) show significant differences depending on the existence of magnetic ions, those of β -(BDA-TTP) $_2$ MCl $_4$ (M =Fe, Ga) are almost identical. The

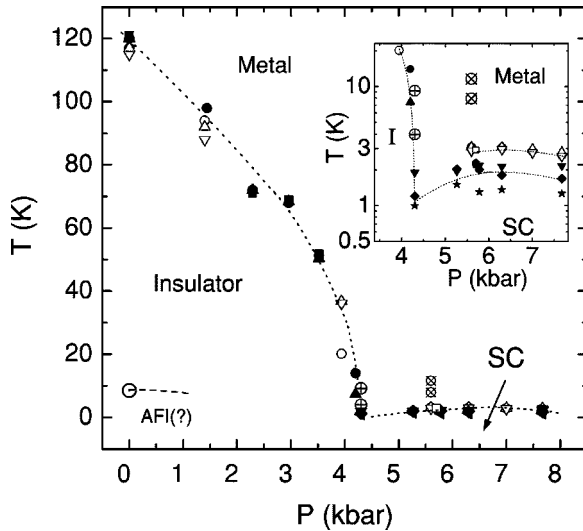


FIG. 2. Temperature-pressure phase diagram of β -(BDA-TTP) $_2$ MCl $_4$ (M =Fe, Ga). Solid symbols are for M =Fe and open symbols for M =Ga. Different symbols indicate different samples. T_{MI} 's below, where superconductivity is also observed, are drawn as \oplus (M =Fe) and \otimes (M =Ga). The AF transition temperature is also shown as \odot . Dotted lines are guides for the eyes. Inset: the log T vs P expanded region near the I - M - SC region.

other (BETS) $_2$ MCl $_4$ (M =Fe, Ga) compounds with a different molecular stacking (κ phase) also show nearly identical ground states.^{25,26}

B. Magnetoresistance and fermiology

Figure 3 shows the MR of β -(BDA-TTP) $_2$ MCl $_4$ (M =Fe, Ga) at T =1.4 K and P =5.7 kbar to 25 T for different field directions, where the M =Fe and M =Ga samples were measured simultaneously in a single pressure cell. For both samples, the upper critical field H_{c2} is higher when the field is parallel to the conducting planes ($B \perp b$), and Shubnikov-de Haas (SdH) oscillations are observed at high fields when $B \parallel b$. Only one SdH frequency and its harmonics were observed in the fast Fourier transform (FFT) spectrum for both compounds. The angular dependence of the SdH frequency follows $1/\cos \theta$ as shown in the inset, indicating a closed orbit, quasi-two-dimensional Fermi surface for both samples.²⁷ The SdH frequency is found to be slightly larger for the M =Fe samples at the same pressure. Some interesting features found in the MR of M =Fe samples are (i) an abrupt drop of MR around 5 T (defined as B^* hereafter), (ii) an overall negative MR to about 20 T (defined as B^{**} hereafter), and (iii) a broad upturn above B^{**} . The abrupt drop of MR at B^* is angle dependent and most significant for the field perpendicular to the conducting planes. We will discuss these features in detail below.

Figure 4 shows MR of β -(BDA-TTP) $_2$ MCl $_4$ (M =Fe, Ga) measured at higher fields (to 33 T) and lower temperatures and at the highest pressure (7.7 kbar) in this work. The overall features of the MR observed in Fig. 3 were reproduced with more pronounced SdH oscillations and MR anomalies. The SdH oscillations are always more prominent

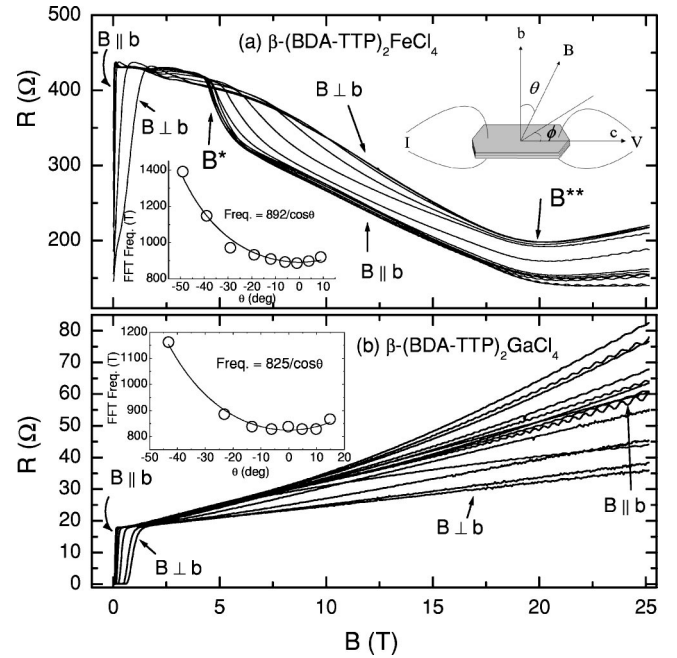


FIG. 3. Magnetoresistance of β -(BDA-TTP) $_2$ MCl $_4$: (a) M =Fe and (b) M =Ga, at P =5.7 kbar and T =1.4 K at different angles. The contact configuration and definition of angles are also shown. Inset: the SdH frequency as a function of θ fit to $F_0/\cos \theta$.

in M =Ga samples, and the Dingle temperature T_D of M =Ga is generally smaller than for the M =Fe samples: T_D is about 1 K for M =Ga, and 4 K for M =Fe. The inset of Fig. 4(b) shows a Dingle plot²⁷ based on 7.7 kbar data shown here. For the M =Fe samples, although the SdH oscillation amplitude is very small below 20 T, there is no evidence for any deviation from the LK behavior as the field passes through B^{**} . Since there is no significant difference of the residual resistance ratio (RRR) between two compounds (~ 13 for both samples shown here), we speculate that the larger T_D of M =Fe salts can be ascribed to the influence of magnetic moments. From the temperature-dependent SdH oscillations amplitudes, the effective cyclotron mass (m_c^*) can be obtained using the Lifshitz-Kosevich (LK) formula.²⁷ The SdH frequency and m_c^* at different pressures are summarized in Fig. 5.

The SdH frequency increases linearly with pressure, which indicates an increase of the extremal area of the cylindrical Fermi surface. The effect of hydrostatic pressure is to decrease lattice parameters; hence it increases the volume of the momentum space. The effect of pressure on m_c^* is more complex, since m_c^* includes many-body effects from the electron-electron and electron-phonon interactions as well as the bare band mass term.

In general, m_c^* also decreases with pressure due to the increase of bandwidth (decrease of the density of states), which results in a decrease of both the bare band mass and the electron-phonon interaction. m_c^* decreases with pressure for both M =Fe and M =Ga samples. By extrapolation to zero pressure, the m_c^* values at ambient pressure are estimated to be about $3.4 \pm 0.5 m_e$ and $4.7 \pm 0.3 m_e$ for M =Fe and Ga, respectively. The pressure effect on the density of states may

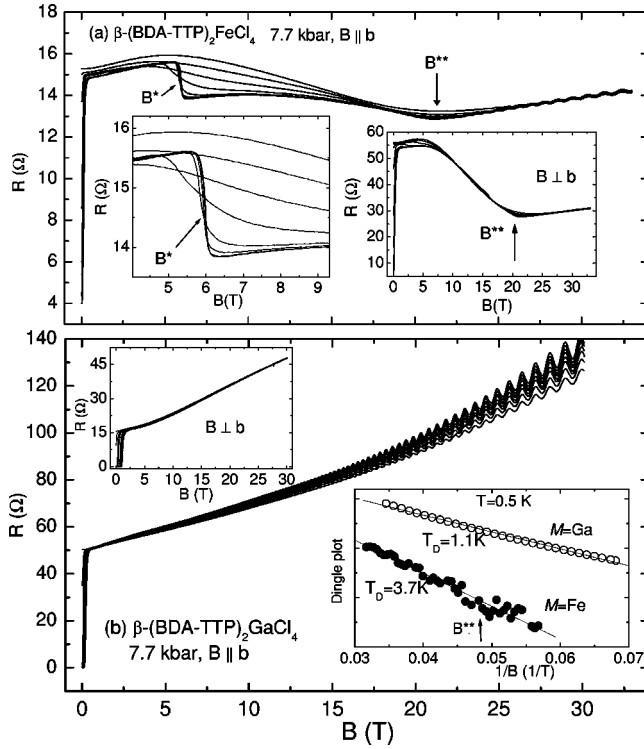


FIG. 4. (a) Magnetoresistance (MR) of β -(BDA-TTP) $_2$ FeCl $_4$ for $B \parallel b$ at $P=7.7$ kbar and at different temperatures 3.5, 2.5, 1.9, 1.5, 1.1, 0.9, 0.7, and 0.5 K from top to bottom. Left inset: expansion around $B=5$ T. Right inset: MR for $B \perp b$ with the same temperature steps. See the text for the definition of B^* and B^{**} . (b) MR of β -(BDA-TTP) $_2$ GaCl $_4$ for the same conditions of (a). Left inset: MR for $B \perp b$. Right inset: Dingle plot [$\ln(AB^{1/2}X^{-1}\sinh X(am_c^*)^{-1})$] vs. B^{-1} , where A is the oscillation amplitude, $X=\alpha m_c^*T/B$ and $\alpha=14.7$ T/K for β -(BDA-TTP) $_2$ MCl $_4$ (M =Fe, Ga). B^{**} denotes the field where MR shows a broad minimum.

also be manifested in changes of T_c ,²⁸ which is significant in many organic conductors [for example, -3 K/kbar for κ -(BEDT-TTF) $_2$ Cu(NCS) $_2$ (Ref. 28)]. In the title compounds, the change of T_c is rather small in the range of pressure measured, and T_c even increases between P_c and 6.5 kbar (inset of Fig. 2). Since the superconductivity is initially stabilized by applying pressure, we may need higher pressure to see the pressure effect on the density of states through the decrease of T_c .

The existence of magnetic ions in a metal is known to enhance the effective mass,^{29,30} which is attributed to a spin fluctuation mechanism. But it is still not clear whether we can ascribe a similar mass enhancement effect in organic conductors with localized magnetic moments. For instance, in κ -(BETS) $_2$ MCl $_4$ compounds, a larger m_c^* was found for M =Fe ($2.8 m_e$) than for M =Ga ($1.2 m_e$).^{25,26} On the other hand, a systematic study done on λ -(BETS) $_2$ Fe $_x$ Ga $_{1-x}$ Cl $_4$ compounds did not show any considerable difference of m_c^* .³¹

The SdH frequencies at ambient pressure can be estimated by a linear extrapolation of the curves shown in Fig. 5, where we obtained 663 T for M =Fe and 628 T for M =Ga. The areas of the closed Fermi surface at ambient pressure were

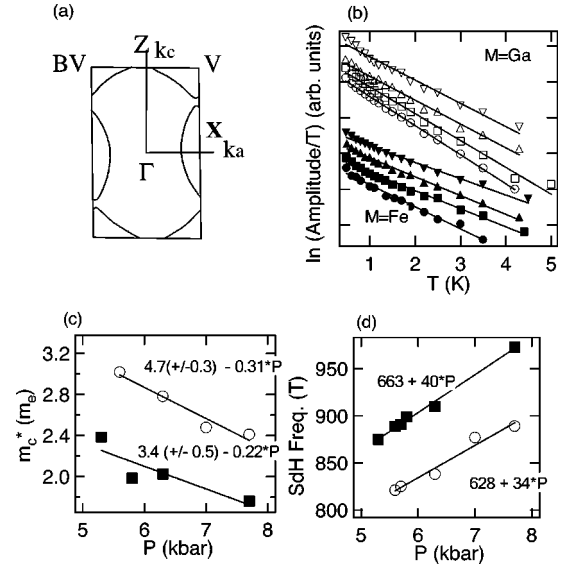


FIG. 5. (a) Theoretical Fermi surface of β -(BDA-TTP) $_2$ MCl $_4$ (M =Fe, M Ga). (b) Mass plots of for M =Fe (solid symbols) and M =Ga (open symbols) at different pressures. The solid lines are linear fits where the slope is proportional to the effective cyclotron mass (m_c^*). Data are offset along the y axis for clarity. Open symbols: M =Ga at 5.6, 6.3, 7.0, and 7.7 kbar from top to bottom. Solid symbols: M =Fe at 5.3, 5.8, 6.3, and 7.7 kbar from top to bottom. (c) Pressure dependence of (m_c^*) for M =Fe (solid symbols) and M =Ga (open symbols). The solid lines are linear fits. (d) Pressure dependence of the SdH frequency for M =Fe (solid symbols) and M =Ga (open symbols). The solid lines are linear fits.

then assumed to be 6.3×10^{14} cm $^{-2}$ and 5.9×10^{14} cm $^{-2}$ for M =Fe and M =Ga, respectively. If we compare this result with a tight binding band calculation result which predicts a closed Fermi surface with 13% of area of the first Brillouin zone (BZ)³² [see Fig. 5(a)], the area of the closed Fermi surface is slightly larger than theory (5.3×10^{14} cm $^{-2}$ for both M =Fe and M =Ga compounds), but this is reasonable since the SdH frequencies were obtained at high pressures. Preliminary angular-dependent magnetoresistance oscillation (AMRO) measurements also indicate similar Fermi surface topologies between the two compounds as expected.³³

It is of note that the theoretical Fermi surface is more like the open orbit and lens orbit topology of the κ -phase materials [i.e., κ -(BEDT-TTF) $_2$ Cu(NCS) $_2$], than it is to other β -type ambient pressure superconductors β -(BDA-TTP) $_2$ X (X =SbF $_6$, AsF $_6$, PF $_6$),¹⁶ even though the same parameters in [Ref. 16] were used for the calculation. This is probably due to the two crystallographically independent donor molecules in the β -(BDA-TTP) $_2$ MCl $_4$ unit cell. The unit cell of the crystal structure of β -(BDA-TTP) $_2$ X (X =SbF $_6$, AsF $_6$, PF $_6$) contains only one donor molecule. Hence the slight deviation of the degeneracy on the X-V zone boundary in the Fermi surface of β -(BDA-TTP) $_2$ MCl $_4$ is attributed to the presence of two independent donor molecules, and this leads to open and closed orbit sections of the FS. The gap between the open and closed Fermi surface is quite large, which is the most direct reason why we could not observe any magnetic breakdown (MB) orbit in MR. The

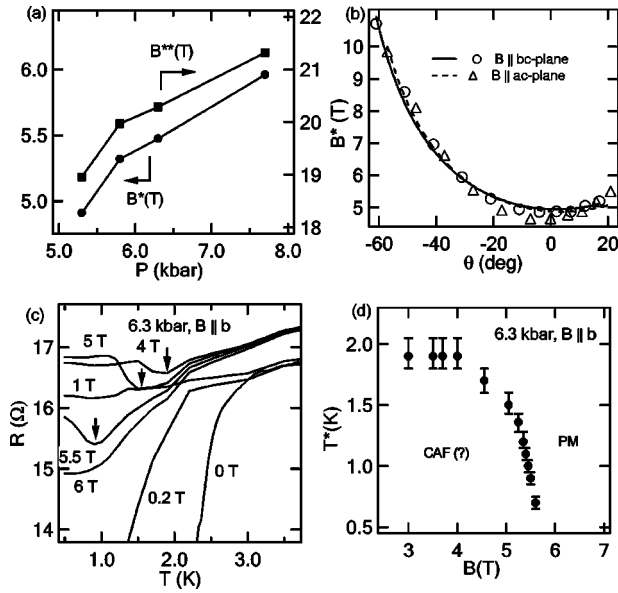


FIG. 6. (a) The pressure dependence of B^* and B^{**} . (b) The angular dependence of B^* for a sample at $P=5.7$ kbar and for two different azimuthal angles $\phi=0$ ($B \parallel bc$ planes) and 90° ($B \parallel bc$ planes). (c) The temperature dependence of resistance at a fixed magnetic field for a β -(BDA-TTP) $_2$ FeCl $_4$ sample at $P=6.3$ kbar and $B \parallel b$. The down arrow indicates T^* where the resistance shows local minimum. (d) The magnetic field dependence T^* from the $R(T)$ curves shown in (c).

band calculation results indicate the MB gap of the title compounds is 28 meV, which is about 5 times larger than κ -(BEDT-TTF) $_2$ Cu(NCS) $_2$ at ambient pressure. Hence, much higher fields are needed to observe the MB orbit, since the magnetic field should satisfy the condition $\hbar\omega_c > \varepsilon_g^2/\varepsilon_F$, where ω_c is the cyclotron frequency eB/mc , ε_g is the MB gap, and ε_F is the Fermi energy.³⁴

In organic conductors with magnetic ions, a negative MR is a common characteristic. Negative MR was observed in κ -(BETS) $_2$ FeBr $_4$ (Refs. 11 and 13) and also in κ -(BETS) $_2$ FeCl $_4$.²⁶ In the κ -(BETS) $_2$ FeCl $_4$ compound, the negative MR is followed by a positive of MR above 30 T, which is similar to the behavior of β -(BDA-TTP) $_2$ FeCl $_4$ above B^{**} . Since the only noticeable difference between β -(BDA-TTP) $_2$ FeCl $_4$ and β -(BDA-TTP) $_2$ GaCl $_4$ is the existence of magnetic ions, the anomalies observed in the MR can be attributed to magnetic interactions between conduction electrons and magnetic ions. The overall negative MR in the M =Fe sample may be explained by the suppression of scattering as the magnetic field gradually aligns paramagnetic spins. For full polarization, the negative MR should saturate. Above the saturation field B^{**} , normal quasi-two-dimensional (Q2D) Fermi surface effects, which produce a positive MR as in the M =Ga case, should determine the magneto-transport behavior at higher fields. The fact that there is no observable hysteresis around B^{**} indicates that the alignment mechanism is paramagnetic rather than ferromagnetic.

In Fig. 6, we summarize the characteristic behavior of the MR anomalies as a function of pressure, field orientation and temperature. Though both B^* and B^{**} increase with pres-

sure [see Fig. 6(a)], the B^* anomaly is more sensitive to temperature and field orientation and also shows hysteretic behavior (data not shown). The B^* anomaly appears only below a critical temperature (~ 2.2 K) and the drop becomes more prominent at lower temperatures. The size of the MR decrease varies from sample to sample ranging from 10% to 15% of resistive value just before the drop. The anisotropy of B^* is shown in Fig. 6(b), where B^* was defined as a minimum of dR/dB curves. B^* follows $1/\cos\theta$ for both the $B \parallel bc$ plane and the $B \parallel ac$ plane, which indicates the field component perpendicular to the conducting planes (ac plane) causes the drop of MR.

Interestingly, a similar behavior of the MR around 5 T was also reported in κ -(BETS) $_2$ FeBr $_4$ (Refs. 11 and 13) and λ -(BETS) $_2$ FeCl $_4$ under 6 kbar.³⁵ In κ -(BETS) $_2$ FeBr $_4$ and λ -(BETS) $_2$ FeCl $_4$ compounds, the resistance drop was attributed to a transition from a canted AF (CAF) phase to a paramagnetic metal (PM) phase.³⁶ For the both compounds, the drop of MR is most significant when the field is perpendicular to the conducting planes as in β -(BDA-TTP) $_2$ FeCl $_4$. But the details of MR behavior differ between compounds. For instance, the angular dependence of the transition field (assigned as B^*) follows $\cos\theta$ for κ -(BETS) $_2$ FeBr $_4$, while B^* is more or less insensitive to the field orientation for λ -(BETS) $_2$ FeCl $_4$. The general behavior of the MR above B^* is also diverse: λ -(BETS) $_2$ FeCl $_4$ shows positive MR, while the MR of κ -(BETS) $_2$ FeBr $_4$ changes from negative to positive as the magnetic field is tilted away from the perpendicular direction. The differences in the angular dependence are puzzling since the easy axes of AF transition at ambient pressure are known to lie in the conducting planes for the compounds mentioned above. As it is most probable that the alignment of local moments is the origin of the MR anomaly, magnetization measurements for pressurized samples are necessary for further investigation.

The temperature dependence of resistance at fixed fields around B^* , which was obtained from field sweeps at different temperatures, is shown in Fig. 6(c). At higher temperatures, $R(T)$ is metallic with similar temperature dependence regardless of the field. But between 3 and 5.5 T, $R(T)$ starts to increase at lower temperatures below T^* showing a non-metallic temperature dependence. The field dependence of T^* is shown in Fig. 6(d), where $T^*(B)$ is suggestive as the phase boundary between paramagnetic metal and CAF phases.

IV. DISCUSSION

The donor molecules of β -(BDA-TTP) $_2$ MCl $_4$ (M =Fe,Ga) are dimerized along the c axis so that the metallic band of the material is effectively half filled. The tight binding calculation also indicates that the donor molecule stacking is rather compressible. For instance, the largest transfer integral is about half that of β -(BEDT-TTF) $_2$ I $_3$ and κ -(BEDT-TTF) $_2$ Cu(NCS) $_2$.¹⁶ Therefore, β -(BDA-TTP) $_2$ MCl $_4$ is prone to a Mott insulator transition when the conduction electron screening is weak, which may be what we see in the TP -phase diagram in Fig. 2. The

suppression of the insulating state by pressure is then due to the increase of the bandwidth (W) with pressure to above a certain W/U (U is the Coulomb correlation) value. This is also *indirectly* supported by the strong pressure dependence of the SdH frequency in this material (a 45% and 40% increase at 7.5 kbar for $M=\text{Fe}$ and Ga , respectively, compared to a 22% increase for $\kappa\text{-(BEDT-TTF)}_2\text{Cu(NCS)}_2$ at the same pressure^{28,37}). We suspect that the conformational distortion of the BDA-TTP molecules from planar geometry leads to the compressible donor packing motifs. That is, a flapping (vertical) motion of the two trimethylene end groups ($-\text{CH}_2\text{CH}_2\text{CH}_2-$) with respect to the molecular plane causes the outer six-membered rings to become non-planar and can take on a number of conformations. An analogous situation can be encountered in the BEDT-TTF-based compounds; however, in this case, two “twist” conformations (the so-called “eclipsed” and “staggered” configurations) are present in the ethylene end groups ($-\text{CH}_2\text{CH}_2-$) of the BEDT-TTF molecule. Taking into account the high compressibility, the conformational change by the “flapping” may be relatively flexible and sensitive to the pressure in comparison with that by “twisting.” With the absence of SdH oscillations corresponding to the magnetic breakdown orbit in the title compounds,³⁷ structural analysis will be necessary to clarify this issue.

The proximity of the insulator, superconductor, and metal ground states around 4.3 kbar (inset of Fig. 2) is intriguing. Here, the metal insulator transition and the SC critical temperature are observed in a narrow temperature range. For the $\beta\text{-(BDA-TTP)}_2\text{FeCl}_4$ compound, the AF phase should lie below the paramagnetic Mott insulator phase in the TP -phase diagram and may also share a boundary with the SC state. Since the proximity of the AF and SC states is observed in several high T_c superconducting oxides and organic superconductors, a complete phase diagram of $\beta\text{-(BDA-TTP)}_2\text{FeCl}_4$, including a pressure dependence of T_N , should be revealing. The coexistence of the AF and SC states is reported in $\kappa\text{-(BEDT-TTF)}_2\text{Cu[N(CN)}_2\text{Cl]}$,³⁸ and in the $\kappa\text{-(BETS)}_2\text{FeBr}_4$ compound,^{11–13} where a small resistance drop at T_N was observed. In the $\beta\text{-(BDA-TTP)}_2\text{FeCl}_4$ samples, we did not observe any decisive changes in resistance measurements around T_c attributable to an AF transition. But the anomaly observed in MR around $B^* = 5$ T suggests that AF ordering may also exist for the superconductor $\beta\text{-(BDA-TTP)}_2\text{FeCl}_4$.

When the Mott insulator state is suppressed, but is still at an intermediate value of W/U , the ground states may be determined by the strength of magnetic interactions J between conduction electrons and localized magnetic moments.¹⁴ This effect is manifest in the $\lambda\text{-(BETS)}_2\text{MCl}_4$ ($M=\text{Fe, Ga}$) compounds, where the ground state is either SC ($M=\text{Ga}$) or insulator ($M=\text{Fe}$), depending on the presence of magnetic moments. But the similarity of the phase diagram in $\beta\text{-(BDA-TTP)}_2\text{MCl}_4$ ($M=\text{Fe, Ga}$) suggests that J is much smaller than that of $\beta\text{-(BDA-TTP)}_2\text{FeCl}_4$. $\kappa\text{-(BETS)}_2\text{FeBr}_4$ may be also considered to have a small J considering its AF metal/SC ground state. Mori and Katsuhara estimated the J for several organic conductors using the extended Hückel type calculation.³⁹ In this

model, the π - d interactions can be written as $J = -2t^2/\Delta$, where t is the transfer integrals between the donor HOMO (highly occupied molecular orbitals) and anion d -orbitals and Δ is the energy difference between them. Naively, the J value will be larger for greater overlap (shorter intermolecular distance) between donor and anion molecules. Indeed, at ambient conditions, the closest distances between FeCl_4 and BDA-TTP molecules are between the Cl and S atoms located in the outer six-membered rings [3.837(3) Å and 3.740(5) Å], which are still longer than van der Waals radii of chlorine and sulfur atoms (3.55 Å). On the other hand, in $\lambda\text{-(BETS)}_2\text{FeCl}_4$ compounds, many short Cl-S (and also Cl-Se located in the inter-six-membered rings) contacts are found that are shorter than the van der Waals radii, which may give stronger interactions between conduction electrons and magnetic moments.^{3,12}

Although perhaps weaker than in other organic-magnetic compounds, the effect of magnetic interactions in the $M=\text{Fe}$ system are observed in quantum oscillations (increased T_D) and in additional features of the MR. The field dependence of the SdH oscillation, especially in the region where MR is negative, may reveal effects of additional spin scattering, since the spin scattering tends to be suppressed with increased field. In the current study, it is not conclusive whether the effect is observable since the SdH oscillations are very weak below B^{**} [see the lower inset of Fig. 4(b)]. Nevertheless, the increased T_D for the $M=\text{Fe}$ sample indicates the spin-dependent scattering should be still relevant even when spins are completely aligned and periodically arranged. The transition from a negative to a positive MR at B^{**} is likely to have the same origin as in other organic conductors with magnetic ions. But the abrupt drop of MR around 5 T when the field is perpendicular to the conducting planes is still not well understood. Bulk magnetization or magnetic resonance measurements may reveal magnetic transitions, which will be useful to understand the observed behavior. Nevertheless, the pressure dependence of B^* and B^{**} [see Fig. 6(a)] can be explained by the simple argument above, i.e., J increases with greater overlap between molecules under pressure.

Finally, we want to address a possibility of the FISC state in a $\beta\text{-(BDA-TTP)}_2\text{FeCl}_4$ compound. The FISC state was found in two organic superconductors at present, and it was suggested that it may be an inherent property in a layered superconductor with magnetic ions.¹⁰ The FISC state was explained by the Jaccarino-Peter mechanism, where electrons experience an effective magnetic field (H_{eff}) compensated by an exchange field ($H_{\text{eff}}=H-H_e$, where H_e is an exchange field by magnetic moments due to antiferromagnetic exchange).^{6,7,14} To observe this phenomenon, magnetic fields should be aligned in the layers to suppress orbital effects that will destroy superconductivity even at smaller fields. When the orbital effect is suppressed, superconductivity may be observed if $|H-H_e| < H_p$ (H_p is the Pauli paramagnetic limit). The existence of H_e has been measured by the spin-split SdH oscillation frequencies, or in principle by electron spin resonance (ESR).¹⁴ For both $\kappa\text{-(BETS)}_2\text{FeBr}_4$ and $\lambda\text{-(BETS)}_2\text{FeCl}_4$ compounds, H_e was estimated to be about 10 and 32 T, respectively, from SdH oscillation

measurements,^{11,13,40} which agree well with the optimal field to observe FISC states in those compounds. On the other hand, in β -(BDA-TTP)₂FeCl₄ samples, only a single SdH frequency was observed and no clear evidence of the FISC has been found. The frequency split in the SdH oscillations (δF) by an exchange field can be written as $\delta F = g^* m_c^* H_e$, where g^* is renormalized g factor. Since the Dingle temperature of this compound is rather large (~ 4 K) and with small m_c^* ($\sim 2 m_e$) and probably small H_e also, lower temperature and/or higher field may be needed to observe δF in this compound.

In summary, we have investigated the TP -phase diagram and electronic structure of β -(BDA-TTP)₂MCl₄ ($M = \text{Ga, Fe}$). The ground state and the Fermi surface of both compounds are very sensitive to pressure, which may be a general character of BDA-TTP-based organic conductors due to the highly nonplanar donor structure. The insulating state is suppressed by pressure, resulting in a SC state above 4.5 kbar. The significant change of SdH frequency with pressure suggests that the Mott insulating phase is suppressed by increased bandwidth. The overall TP -phase diagram and fer-

miology are quite similar in the $M = \text{Fe}$ and Ga compounds, which can be attributed to a small J in $M = \text{Fe}$ compound. Even with those similarities, the magnetoresistance appears to be sensitive even in the limit of small J , and hence the effect of magnetic interaction is manifested in several observations: (i) the SC transition is less prominent for the $M = \text{Fe}$ compound (broader transition and smaller T_c); (ii) the larger Dingle temperature and the overall negative MR for the $M = \text{Fe}$ compound can be attributed to an additional scattering by magnetic moments; and (iii) the abrupt drop of MR around 5 T, which is highly sensitive to temperature and magnetic field orientation, indicates the presence of anisotropic magnetic order in the $M = \text{Fe}$ compound, where AF order may even be present in the superconducting state.

ACKNOWLEDGMENTS

We thank Ross H. McKenzie who brought our attention to the title compounds. This work is supported in part by NSF-DMR 0203532. The NHMFL is supported by a contractual agreement between NSF and the state of Florida.

-
- ¹A. Kobayashi, T. Udagawa, H. Tomita, T. Naito, and H. Kobayashi, *Chem. Lett.* **1993**, 2179.
- ²F. Goze, V. N. Laukhin, L. Brossard, A. Audouard, J. P. Ulmet, S. Askenazy, T. Naito, H. Kobayashi, A. Kobayashi, M. Tokumoto, and P. Cassoux, *Physica B* **211**, 290 (1995).
- ³H. Kobayashi, H. Tomita, T. Naito, A. Kobayashi, F. Sakai, T. Watanabe, and P. Cassoux, *J. Am. Chem. Soc.* **118**, 368 (1996).
- ⁴H. Kobayashi, H. Akutsu, and E. Arai, *Phys. Rev. B* **56**, R8526 (1997).
- ⁵L. Brossard, R. Clerac, C. Coulon, M. Tokumoto, T. Ziman, D. K. Petrov, V. N. Laukhin, M. J. Naughton, A. Audouard, F. Goze, A. Kobayashi, H. Kobayashi, and P. Cassoux, *Eur. Phys. J. B* **1**, 439 (1998).
- ⁶S. Uji, H. Shinagawa, T. Terashima, T. Yakabe, Y. Terai, M. Tokumoto, A. Kobayashi, H. Tanaka, and H. Kobayashi, *Nature (London)* **410**, 908 (2001).
- ⁷L. Balicas, J. S. Brooks, K. Storr, S. Uji, M. Tokumoto, H. Tanaka, H. Kobayashi, A. Kobayashi, V. Barzykin, and L. P. Gor'kov, *Phys. Rev. Lett.* **87**, 067002 (2001).
- ⁸H. Fujiwara, H. Kobayashi, E. Fujiwara, and A. Kobayashi, *J. Am. Chem. Soc.* **124**, 6816 (2002).
- ⁹M. A. Tanatar, M. Suzuki, T. Ishiguro, H. Fujiwara, and H. Kobayashi, *Physica C* **388**, 613 (2003).
- ¹⁰T. Konoike, H. Fujiwara, B. Zhang, H. Kobayashi, M. Nishimura, S. Yasuzuka, K. Enomoto, and S. Uji, *Proceedings of ISCOM 2003, Port-Bourgenay, France*, and *[J. Phys. IV* **44**, 223 (2004)].
- ¹¹L. Balicas, J. S. Brooks, K. Storr, D. Graf, S. Uji, H. Shinagawa, E. Ojima, H. Fujiwara, H. Kobayashi, A. Kobayashi, and M. Tokumoto, *Solid State Commun.* **116**, 557 (2000).
- ¹²H. Fujiwara, E. Fujiwara, Y. Nakazawa, B. Zh. Zarymbetov, K. Kato, H. Kobayashi, A. Kobayashi, M. Tokumoto, and P. Cassoux, *J. Am. Chem. Soc.* **123**, 306 (2001).
- ¹³S. Uji, H. Shinagawa, Y. Terai, T. Yakabe, C. Terakura, T. Terashima, L. Balicas, J. S. Brooks, E. Ojima, H. Fujiwara, H. Kobayashi, A. Kobayashi, and M. Tokumoto, *Physica B* **298**, 557 (2001).
- ¹⁴O. Cépas, R. H. McKenzie, and J. Merino, *Phys. Rev. B* **65**, R100502 (2002).
- ¹⁵H. Tanaka, T. Adachi, E. Ojima, H. Fujiwara, K. Kato, H. Kobayashi, A. Kobayashi, and P. Cassoux, *J. Am. Chem. Soc.* **121**, 11243 (1999).
- ¹⁶J. Yamada, M. Watanabe, H. Akutsu, S. Nakatsuji, H. Nishikawa, I. Ikemoto, and K. Kikuchi, *J. Am. Chem. Soc.* **123**, 4174 (2001).
- ¹⁷J. Yamada, M. Watanabe, H. Anzai, H. Nishikawa, I. Ikemoto, and K. Kikuchi, *Angew. Chem., Int. Ed.* **38**, 810 (1999).
- ¹⁸E. S. Choi, E. Jobiliong, A. Wade, E. Goetz, J. S. Brooks, J. Yamada, T. Mizutani, T. Kinoshita, and M. Tokumoto, *Phys. Rev. B* **67**, 174511 (2003).
- ¹⁹K. Kikuchi, H. Nishikawa, I. Ikemoto, T. Toita, H. Akutsu, S. Nakatsuji, and J. Yamada, *J. Solid State Chem.* **168**, 503 (2002).
- ²⁰J. Yamada, T. Toita, H. Akutsu, S. Nakatsuji, H. Nishikawa, I. Ikemoto, and K. Kikuchi, *Chem. Commun. (Cambridge)* **2001**, 2538.
- ²¹M. Tokumoto, K. Ishii, H. Tanaka, H. Akutsu, J. Yamada, E. S. Choi, J. S. Brooks, and K. Ishida, *Proceedings of ISCOM 2003, Port-Bourgenay, France [J. Phys. IV* **44**, 385 (2004)].
- ²²Y. Oshima, J. S. Brooks, and J. Yamada (unpublished).
- ²³J. Yamada, T. Toita, H. Akutsu, S. Nakatsuji, H. Nishikawa, I. Ikemoto, K. Kikuchi, E. S. Choi, D. Graf, and J. S. Brooks, *Chem. Commun. (Cambridge)* **2003**, 2230.
- ²⁴M. I. Eremets, *High Pressure Experimental Methods* (Oxford University Press, Oxford, 1996).
- ²⁵H. Tajima, A. Kobayashi, T. Naito, and H. Kobayashi, *Solid State Commun.* **98**, 755 (1996).
- ²⁶N. Harrison, C. H. Mielke, D. G. Rickel, L. K. Montgomery, C. Gerst, and J. D. Thompson, *Phys. Rev. B* **57**, 8751 (1998).
- ²⁷J. Wosnitzer, *Fermi Surfaces of Low-dimensional Organic Metals*

- and Superconductors* (Springer, Berlin, 1996).
- ²⁸J. Caulfield, W. Lubczynski, F. L. Pratt, J. Singleton, D. Y. K. Ko, W. Hayes, M. Kurmoo, and P. Day, *J. Phys.: Condens. Matter* **6**, 2911 (1994).
- ²⁹R. J. Trainor, M. B. Brodsky, and H. V. Culbert, *Phys. Rev. Lett.* **34**, 1019 (1975).
- ³⁰A. LeR. Dawson, D. H. Ryan, and David V. Baxter, *Phys. Rev. B* **54**, 12238 (1996).
- ³¹S. Uji, C. Terakura, T. Terashima, T. Yakabe, and Y. Terai, M. Tokumoto, A. Kobayashi, F. Sakai, H. Tanaka, and H. Kobayashi, *Phys. Rev. B* **65**, 113101 (2001).
- ³²J. Yamada, Proceedings of ISCOM 2003, Port-Bourgenay, France, [*J. Phys. IV* **144**, 439 (2004)].
- ³³E. S. Choi, J. S. Brooks, and J. Yamada (unpublished).
- ³⁴E. I. Blount, *Phys. Rev.* **126**, 1636 (1962).
- ³⁵Y. J. Jo, Haeyong Kang, T. Tanaka, M. Tokumoto, A. Kobayashi, H. Kobayashi, S. Uji, and W. Kang, Proceedings of ISCOM 2003, Port-Bourgenay, France [*J. Phys. IV* **144**, 323 (2004)].
- ³⁶For κ -(BETS)₂FeBr₄, magnetization measurements (Ref. 12) indicate a complete spin alignment around 6 T, while gradual alignment of spins above 6 T are suggested from MR measurements in Refs. 11 and 13.
- ³⁷The pressure dependence on the SdH frequency of the magnetic breakdown (MB) orbit is more relevant to the compressibility. Since the MB orbit represents the full first Brillouin zone area, its frequency is directly related to the in-plane lattice constants. In Ref. 28, the increase rate of SdH frequency corresponding to the MB orbit was found to be smaller than that of the closed Fermi surface.
- ³⁸S. Lefebvre, P. Wzietek, S. Brown, C. Bourbonnais, D. Jérôme, C. Mézière, M. Fourmigué, and P. Batail, *Phys. Rev. Lett.* **85**, 5420 (2000).
- ³⁹T. Mori and M. Katsuhara, *J. Phys. Soc. Jpn.* **71**, 826 (2002).
- ⁴⁰S. Uji, H. Shinagawa, C. Terakura, T. Terashima, T. Yakabe, Y. Terai, M. Tokumoto, A. Kobayashi, H. Tanaka, and H. Kobayashi, *Phys. Rev. B* **64**, 024531 (2001).